Far East Journal of Mathematical Sciences (FJMS)

Published Online: May 2014
Available online at http://pphmj.com/journals/fjms.htm
Volume 87, Number 1, 2014, Pages 23-35

A NOVEL MODEL DETERMINATION OF BREAST CANCER STAGE USING PHYSICAL PARAMETER

Anak Agung Ngurah Gunawan

Department of Physics
University of Udayana at Bali
Indonesia
e-mail: agung1962sp@yahoo.co.id

Abstract

This article determines the stage of breast cancer with a new method using mathematical equation models with physical parameters. To determine the stage of breast cancer, a model has been developed by the method of Tumor Node Metastasis (TNM) and Scarff-Bloom-Richardson. In this study, we have used mathematical equation models with physical parameters to determine the probability of gray-level pair at a certain distance. In a previous research, we managed to determine the histological type of breast cancer using the physical parameters. The proposed approach has been tested on 15 mammograms new patients of Dr. Soetomo Hospital, Indonesia. The results showed that the use of physical parameters was actually able to predict the stage of breast cancer with a sensitivity of 86,67% on the footage 5×5 cm and $\alpha = 5\%$.

1. Introduction

Many methods of early detection of breast cancer have been developed such as texture coding [1], edge detection [2], adaptive *k*-means clustering

Received: August 16, 2013; Accepted: October 8, 2013
2010 Mathematics Subject Classification: 92C55.
Keywords and phrases: stage, breast cancer, mammogram, physical parameter.

[3], self similar fractal [4], fractal feature [5], neural network [6], Kekre's [7], SVM classifier [8], texture resemblance marker [9], extraction [10], accurate method [11], contour description [12], bilateral asymmetry [13], orthogonal polynomials model [14], the dual tree complex [15], Gabor features [16], fuzzy clustering [17], *k*-means and fuzzy *c*-means [18], vector quantization technique [19], Kohonen SOM and LVQ network [20], entropy Sallis *Q* and a type II fuzzy [21], foveal method [22] and wavelet [23]. However, these methods only detect the presence of microcalcification course and not the breast cancer staging. In a previous study, we have succeeded in classifying types of breast cancer histology using physical parameters of the sensitivity of 86.36% on a 5×5 cm samples with $\alpha = 5\%$ [24].

The paper is organized as follows: Section 2 discusses the interaction of radiation with breast cancer, Section 3 discusses the physical parameters, Section 4 discusses the logistic regression mapping function and Section 5 discusses multinomial linear regression function as the outcome of the stage type. Section 6 discusses the result and discussion and last, conclusions are discussed in Section 7.

2. Radiation Interaction with Breast Cancer

The intensity of the radiation beam on breast cancer is partly absorbed and partly transmitted. The intensity of the transmitted radiation beam of density is dependent upon the breast cancer. As the breast density becomes greater, the more the intensity of the light is absorbed or the less the intensity of the transmitted beam. The less the intensity of the transmitted light, the closer the gray-level mammogram films gets to a white color or higher pixel intensity values. Relationship intensity of the light transmitted by the density of breast cancer can be written as follows:

$$I_t = I_0 e^{-\mu L}, \tag{2.1}$$

where I_t, I_0, μ, L are the intensity of each beam that is being passed, the intensity of initial light, the absorption coefficient and the density of breast cancer, respectively.

3. Physical Parameters

Each level of malignancy disease has different patterns of pixel intensities. Of these patterns are probabilities pair gray-level at a certain distance. Pair of gray-level probability at any distance can be determined by lack of uniformity (entropy), sharpness structural variations (contrast), structural uniformity (angular second moment), the local homogeneity (inverse difference moment), linear dependence (correlation), authenticity properties (mean), density (deviation), lack of uniformity of the distribution of probability of occurrence gray-level pair at a certain distance (entropy of H_{diff}), structural uniformity of the distribution of probability of occurrence gray-level pair at a certain distance (angular second moment of H_{diff}) and the nature of the authenticity of the pair probability distribution of gray-level events at a certain distance (mean H_{diff}) as follows [24, 25]:

$$Entropy\,(E) = -\sum_{y_q=y_1}^{y_t}\sum_{y_r=y_1}^{y_t}[H(y_q,\ y_r,\ d)]\log[H(y_q,\ y_r,\ d)], \quad (3.1)$$

$$Contrast\,(C) = \sum_{y_q=y_1}^{y_t}\sum_{y_r=y_1}^{y_t}(y_q - y_r)^2 H(y_t,\ y_r,\ d), \quad (3.2)$$

$$Angular\ second\ moment\ (ASM)$$

$$= \sum_{y_q=y_1}^{y_t}\sum_{y_r=y_1}^{y_t}[H(y_q,\ y_r,\ d)]^2, \quad (3.3)$$

$$Moment\ differential\ inverse\ (MDI)$$

$$= \sum_{y_q=y_1}^{y_t}\sum_{y_r=y_1}^{y_t}\left[\frac{H(y_q,\ y_r,\ d)}{1+(y_q - y_r)^2}\right] \quad (3.4)$$

for $y_r \neq y_q$,

$$Correlation\ (Corr)$$

$$= \frac{\sum_{y_q=y_1}^{y_t}\sum_{y_r=y_1}^{y_t} y_q y_r H(y_q,\ y_r,\ d) - \mu H_m(y_q,\ d)\mu H_m(y_r,\ d)}{\sigma H_m(y_q,\ d)\sigma H_m(y_r,\ d)} \quad (3.5)$$

with

$$H_m(y_q, d) = \sum_{y_r = y_1}^{y_t} H(y_q, y_r, d), \tag{3.6}$$

$$H_m(y_r, d) = \sum_{y_q = y_1}^{y_t} H(y_q, y_r, d), \tag{3.7}$$

$$Mean(M) = \sum_{y_q = y_1}^{y_t} y_q H_m(y_q, d), \tag{3.8}$$

$$Deviation(D) = \sqrt{\sum_{y_q = y_1}^{y_t} \left[y_q - \sum_{y_p = y_1}^{y_t} y_p H_m(y_p, d) \right]^2 H_m(y_q, d)}, \tag{3.9}$$

$$H_{diff}(i, d) = \sum_{y_q = | y_q - y_r | = 1}^{y_t} \sum_{y_r = y_1}^{y_t} H(y_q, y_r, d), \tag{3.10}$$

$$Entropy\ of\ H_{diff}(EHD) = -\sum_{i = i_1}^{i_t} H_{diff}(i, d) \log H_{diff}(i, d), \tag{3.11}$$

$$ASM\ of\ H_{diff}(i, d)(ASMHD) = \sum_{i = i_1}^{i_t} [H_{diff}(i, d)]^2, \tag{3.12}$$

$$Mean\ of\ H_{diff}(MHD) = \sum_{i = i_1}^{i_t} iH_{diff}(i, d), \tag{3.13}$$

where y_q, y_r, d are the gray-level pixel value of unity, the value of the second pixel gray-level and the distance between the two pixels with pixels unity, respectively. $H(y_q, y_r, d)$ is a second-order histogram that describes the distribution of probability of occurrence of a pair of gray-level.

4. Logistic Regression Mapping Function

Review the following probability function:

$P_r(Y)$ and $Y = f(X)$, where the dependent variable that is bound to free variables $\{X_i\}$, and X_i are linearly independent with X_j that is

$X_i \neq \sum_j a_j X_j$, where Y is output category, e.g., $y = 0$, stage 1 category, $y = 1$, stage 2 category and so on, $y = k$, particular category.

This form is multinomial or multiple linear rate.

Review of the logistic function (logic) as follows [24]:

$$logic\{P_r(Y = 1| X)\} = log\left\{\frac{P_r(Y = 1| X)}{1 - P_r(Y = 1| X)}\right\}$$

$$\cong \ln\left\{\frac{P_r(Y = 1| X)}{1 - P_r(Y = 1| X)}\right\} = Y. \tag{4.1}$$

Further, $Y : \{Z_1, Z_2, Z_3, Z_4\}$ with $X : \{all\ of\ entropies\}$.

For example, the category $Y = Z_k$

$$\ln\left\{\frac{P_r(Y = 1| X)}{1 - P_r(Y = 1| X)}\right\} = Z_k. \tag{4.2}$$

Note. Use of functional in natural logarithm related to qualitative mapping (entropy) to qualitative (stage types of breast cancer), which does not satisfy the normal Gaussian, statistically,

$$\frac{P_r(Y = 1| X)}{1 - P_r(Y = 1| X)} = e^{Z_k} \text{ or } \frac{1 - P_r(Y = 1| X)}{P_r(Y = 1| X)} = e^{-Z_k} \text{ to obtain:}$$

$$1 - P_r(Y = 1| X) = P_r(Y = 1| X)e^{-Z_k},$$

$$P_r(Y = 1| X)\{1 + e^{-Z_k}\} = 1,$$

$$P_r(Y = 1| X) = \frac{1}{\{1 + e^{-Z_k}\}}, \tag{4.3}$$

and $P_r(Y = 1| X)$ as a multinomial logistic regression of statistical model.

For example $\{Y = Z_k\}_{k=1, 2}$, it will be found in all categories $\sum_{k=1}^{2} P_r(Z_k = 1| X) = 1,$ to

$$\{Z_k = 1\}\begin{Bmatrix} Z_1 = 1,\ stage\, 1,\ detected \\ Z_2 = 1,\ stage\, 2,\ detected \\ Z_3 = 1,\ stage\, 3,\ detected \end{Bmatrix},$$

$$P_r(Z_1 = 1 | X) = \frac{1}{\{1 + e^{-Z_1}\}}, \tag{4.4}$$

$$P_r(Z_2 = 1 | X) = \frac{1}{\{1 + e^{-Z_2}\}}, \tag{4.5}$$

$$P_r(Z_3 = 1 | X) = \frac{1}{\{1 + e^{-Z_3}\}} \tag{4.6}$$

and because the fulfillment of all categories/stages into force,

$$\sum_{k=1}^{4} P_r(Z_k = 1 | X) = 1,$$

$$P_r(Z_1 = 1 | X) + P_r(Z_2 = 1 | X) + P_r(Z_3 = 1 | X) = 1, \text{ until}$$

$$P_r(Z_1 = 1 | X) = 1 - P_r(Z_2 = 1 | X) - P_r(Z_3 = 1/X),$$

$$P_r(Z_1 = 1 | X) = 1 - \left[\frac{1}{\{1 + e^{-Z_2}\}}\right] - \left[\frac{1}{\{1 + e^{-Z_3}\}}\right]. \tag{4.7}$$

5. Linear Regression Multinomial Function as an Outcome of the Stage Type

Review the following linear regression [24]:

$$Z_k = Z_{k0} + \left\{\sum_{k,\ j=1}^{n} B_{kj}\ Entr_j\right\} + \text{Bkn. MeanHd10}, \tag{5.1}$$

Z_k is the outcome/impact of a number of $\{Entr_j\}$,

Z_{k0} is the intersection/intersection of the axis or the initial value of outcome, $Z_k = Z_{k0}$.

For the tribe $\left\{\sum_{k,\ j=1}^{n} B_{kj}\ Entr_j\right\} + \text{Bkn. MeanHd10} = 0,$

$\sum_{k,\ j=1}^{n} B_{kj}\ Entr_j$ is a nuisance parameter/variable-free number $\{Entr_j\}$ the rank of 1 (one) or linear,

Bkn.MeanHd10 is the correction factor by the number of outcome $\{Entr_j\}$.

For example:

$$Z_2 = Z_{20} + \left\{\sum_{2,\ j=1}^{n} B_{2j}\ Entr_j\right\} + \text{B2n. MeanHd10}, \tag{5.2}$$

$$Z_3 = Z_{30} + \left\{\sum_{3,\ j=1}^{n} B_{3j}\ Entr_j\right\} + \text{B3n. MeanHd10}. \tag{5.3}$$

These are illustrated in Figure 1 as follows:

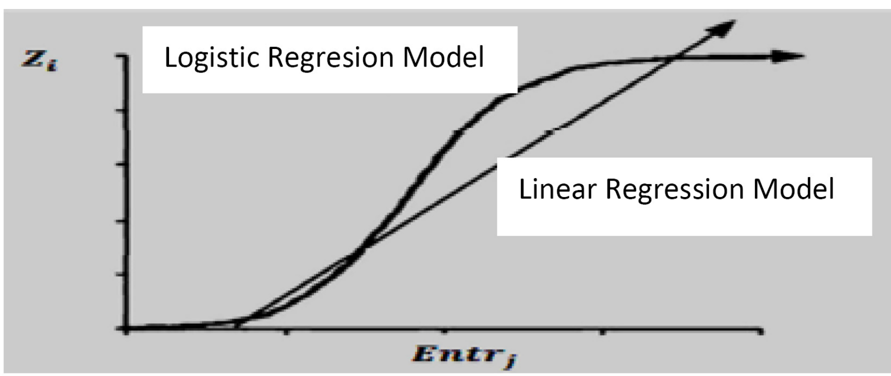

Figure 1. Linear regression model and logistic regression model.

6. Results and Discussion

Figures 2(a), 2(b) and 2(c) are consecutive mammogram pictures of stage 1, stage 2 and stage 3.

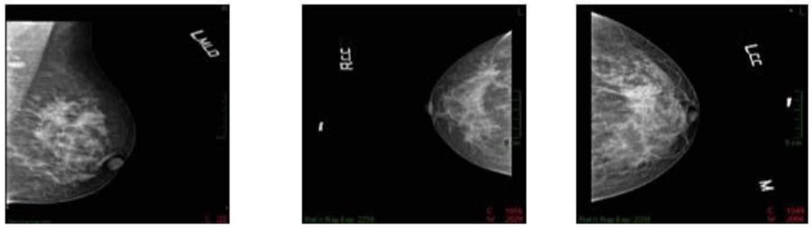

(a) (b) (c)

Figure 2. (a) Stage 1, (b) Stage 2 and (c) Stage 3. All the mammographic images are collected from the data base computer at radiodiagnostic Dr. Soetomo Hospital Indonesia, these images of mammographic labelling Kodak brand, type 6900 laser imager dryview data prints of mammographic films and it is placed in the direct view 975 CR. Images saved in bmp format and sampled with a size of $5 \times 5\,\text{cm}$.

Table 1. Range value of physical parameter stage 1, stage 2 and stage 3

Variable Fisis film	Stage 1	Stage 2	Stage 3
EHD [7]	1.73607-1.94205	1.53297-1.99567	1.47486-1.97046
EHD [8]	1.75712-1.96550	1.54760-2.03515	1.47486-1.99232
EHD [9]	1.77505-1.98493	1.55487-2.06837	1.48628-2.01004
EHD [10]	1.79126-2.00308	1.56675-2.09662	1.49883-2.02729
ASMHD [1]	0.03226-0.04507	0.01040-0.06264	0.02541-0.05055
ASMHD [2]	0.02382-0.03552	0.01921-0.09318	0.01996-0.04772
ASMHD [3]	0.01979-0.03084	0.01885-0.08648	0.01713-0.04533
ASMHD [4]	0.01727-0.02786	0.01780-0.07929	0.01544-0.04395
ASMHD [5]	0.01551-0.02572	0.01577-0.07357	0.01418-0.04331
ASMHD [6]	0.01426-0.02412	0.01420-0.06847	0.01340-0.04119
ASMHD [7]	0.01333-0.02290	0.01303-0.06259	0.01265-0.04005
ASMHD [8]	0.01259-0.02191	0.01176-0.05828	0.01198-0.03905

ASMHD [9]	0.01200-0.02098	0.01075-0.05382	0.01144-0.03791
ASMHD [10]	0.01151-0.01994	0.00998-0.04819	0.01091-0.03688
MHD [1]	9.92311-13.81787	7.03711-22.00450	8.66159-18.50292
MHD [2]	12.71444-18.85441	8.67398-23.14779	9.19399-23.10747
MHD [3]	14.71335-22.88359	10.03482-25.84119	9.71770-26.75284
MHD [4]	16.34673-26.14803	11.44139-28.45701	9.99301-29.55086
MHD [5]	17.79653-29.10036	12.41866-31.16452	10.23093-32.00988
MHD [6]	19.04117-31.69811	12.73418-34.88744	10.72127-33.90060
MHD [7]	20.13923-33.92885	12.95908-38.22411	11.04172-35.78729
MHD [8]	21.15194-35.91399	13.54083-41.38564	11.29721-37.82326
MHD [9]	22.10252-37.64858	13.72020-44.66617	11.63253-39.52103
MHD [10]	23.03941-39.22549	14.14465-47.98476	12.01704-41.35556

Mode of mathematical equations to determine the stage of breast cancer is as follows:

Z_2 := –893.020 + 195160.164 * ASMHD [2] – 510897.436 * ASMHD [3]

+ 533083.158 * ASMHD [4] – 269158.613 * ASMHD [5]

+ 252132.909 * ASMHD [6] – 1440.363 * ASMHD [7]

– 254114.237 * ASMHD [8] – 272372.401 * ASMHD [9]

+ 327999.228 * ASMHD [10] + 94.046 * MHD [1]

– 108.973 * MHD [2] – 1.364 * MHD [3] + 294.227 * MHD [4]

+ 17.633 * MHD [5] – 2.388 * MHD [6] – 638.598 * MHD [7]

+ 1341.563 * MHD [8] – 1927.761 * MHD [9]

+ 995.082 * MHD [10];

$$
\begin{aligned}
Z_3 := {} & -1512.837 + 148397.141 * \text{ASMHD}[2] - 348864.647 * \text{ASMHD}[3] \\
& + 374023.365 * \text{ASMHD}[4] + 582434.961 * \text{ASMHD}[5] \\
& - 990621.703 * \text{ASMHD}[6] - 1598.515 * \text{ASMHD}[7] \\
& + 122174.826 * \text{ASMHD}[8] - 126994.804 * \text{ASMHD}[9] \\
& + 241438.444 * \text{ASMHD}[10] + 44.331 * \text{MHD}[1] \\
& - 320.941 * \text{MHD}[2] - 3.389 * \text{MHD}[3] + 1645.629 * \text{MHD}[4] \\
& - 74.639 * \text{MHD}[5] - 55.387 * \text{MHD}[6] - 4306.505 * \text{MHD}[7] \\
& + 5360.133 * \text{MHD}[8] - 4033.694 * \text{MHD}[9] \\
& + 1837.766 * \text{MHD}[10];
\end{aligned}
$$

Probability stage $2 := 1/(1 + \text{Exp}(-Z_2));$

Probability stage $3 := 1/(1 + \text{Exp}(-Z_3));$

Probability stage 1 := 1 – Probability stage 2 – Probability stage 3.

The optimum physical variables to classify breast cancer stage is structural uniformity of the distribution of probability of occurrence gray level pair at a distance of 2, 3, 4, 5, 6, 7, 8, 9, 10 (angular second moment of H_{diff}) and the nature of the authenticity of the pair probability distribution of gray-level events at a distance of 1, 2, 3, 4, 5, 6, 7, 8, 9, 10 (mean H_{diff}).

7. Conclusion

Tests staging breast cancer were done using physical parameters of 15 new patients' mammogram from the Dr. Soetomo Hospital Indonesia. There are 2 errors and 13 truths resulting in a sensitivity value of 86,67% (13/15) on the footage $5 \times 5\,\text{cm}$ and $\alpha = 5\%$. Hence, staging breast cancer using physical parameters indeed improve the performance in diagnosing breast cancer staging. The optimum physical parameters for classifying breast cancer stage is structural uniformity of the distribution of probability of occurrence gray-level pair at a distance of 2, 3, 4, 5, 6, 7, 8, 9, 10 (angular second moment of H_{diff}) and the nature of the authenticity of the pair probability distribution of gray-level events at a distance of 1, 2, 3, 4, 5, 6, 7, 8, 9, 10 (mean H_{diff}).

References

[1] F. Eddaoudi and F. Regragui, Microcalcifications detection in mammographic images using texture coding, Appl. Math. Sci. 5(8) (2011), 381-393.

[2] B. Senthilkumar and G. Umamaheswari, A novel edge detection algorithm for the detection of breast cancer, European Journal of Scientific Research 53(1) (2011), 51-55.

[3] B. C. Patel and G. R. Sinha, An adaptive *k*-means clustering algorithm for breast image segmentation, International Journal of Computer Applications 10(4) (2010), 35-38.

[4] B. C. Patel and G. R. Sinha, Early detection of breast cancer using self similar fractal method, International Journal of Computer Applications 10(4) (2010), 39-42.

[5] D. Sankar and T. Thomas, Fractal features based on differential box counting method for the categorization of digital mammograms, International Journal of Computer Information System and Industrial Management Applications 2 (2010), 11-19.

[6] J. Dheeba and J. G. Wiselin, Detection of microcalcification clusters in mammograms using neural network, International Journal of Advanced Science and Technology 19 (2010), 13-22.

[7] H. B. Kekre, Saylee M. Gharge and Tanuja K. Sarode, Image segmentation of mammographic images using Kekre's proportionate error technique on probability images, International Journal of Computer and Electrical Engineering 2(6) (2010), 1048-1052.

[8] F. Eddaoudi, F. Regragui, A. Mahmoudi and N. Lamouri, Masses detection using SVM classifier based on textures analysis, Applied Mathematical Sciences 5(8) (2011), 367-379.

[9] M. Nielsen, G. Karemore, M. Loog, J. Raundahl, N. Karssemeijer, J. D. M. Otten, M. A. Karsdal, C. M. Vachon and C. Christiansen, A novel and automatic mammographic texture resemblance marker is an independent risk factor for breast cancer, Cancer Epidemiology 35(4) (2011), 381-387.

[10] M. Vasantha, V. S. Bharathi and R. Dhamodharam, Medical image feature, extraction, selection and classification, International Journal of Engineering Science and Technology 2(6) (2010), 2071-2076.

[11] M. Rizzi, M. D. Aloia and B. Castagnolo, An accurate method to assist physicians for breast cancer detection, World Applied Sciences Journal 10(3) (2010), 348-354.

[12] P. H. Tsui, Y. Y. Liao, C. C. Chang, W. H. Kuo, K. J. Chang and C. K. Yeh, Classification of benign and malignant breast tumors by 2-d analysis based on contour description and scatterer characterization, IEEE Transactions on Medical Imaging 29(2) (2010), 513-521.

[13] S. K. Bandyopadhyay, Image processing algorithms for bilateral asymmetry detection - a survey, Journal of Global Research in Computer Science 1(3) (2010), 39-43.

[14] R. Krishnamoorthy, N. Amudhavalli and M. K. Sivakolundu, Identification of microcalcifications with orthogonal polynomials model, International Journal of Engineering Science and Technology 2(5) (2010), 1204-1210.

[15] K. Sujatha and V. C. Sumitha, Dual tree complex with modified complex ridgelets for image denoising in digital mammographic images, Proceedings of the Int. Conf. on Information Science and Applications ICISA, 2010, pp. 507-511.

[16] Y. Zheng, Breast cancer detection with Gabor features from digital mammograms, Algorithms 3 (2010), 44-62.

[17] N. K. Visalakshi, K. Thangaved and R. Parvathi, An intuitionistic fuzzy approach to distributed fuzzy clustering, International Journal of Computer Theory and Engineering 2(2) (2010), 295-302.

[18] N. Singh and A. G. Mohapatra, Breast cancer mass detection in mammograms using *k*-means and fuzzy *c*-means clustering, International Journal Computer Applications 22(2) (2011), 15-21.

[19] H. B. Kekre, Tanuja K. Sarode and Saylee M. Gharge, Tumor detection in mammography images using vector quantization technique, International Journal of Intelligent Information Technology Application 2(5) (2009), 237-242.

[20] Z. Chalabi, N. Berrached, N. Kharchouche, Y. Ghellemallah, M. Mansour and H. Mouhadjer, Classification of the medical images by the kohonen network SOM and LVQ, Journal of Applied Sciences 8(7) (2008), 1149-1158.

[21] Beenamol Mohanalin, P. K. Kalra and N. Kumar, A novel automatic microcalcification detection technique using Tsallis entropy and a type II fuzzy index, Computers and Mathematics with Applications 60 (2010), 2426-2432.

[22] Oh Whi-Vin, Kim KwangGi and Kim Young-Jae, Detection of microcalcifications in digital mammograms using foveal method, J. Kor. Soc. Med. Informatics 15(1) (2009), 165-172.

[23] S. Bouyahia, J. Mbainaibeye and N. Ellouze, Wavelet based microcalcifications detection in digitized mammograms, ICGST-GVIP Journal 8 (2009), 23-31.

[24] A. A. N. Gunawan, Suhariningsih, K. S. P. Triyono and B. Widodo, Determination of physical parameter model for the photo film mammographic X-ray results on the breast cancer histology classification, Int. J. Contemp. Math. Sciences 7(45) (2012), 2235-2244.

[25] A. P. Dhawan, Y. Chitre, C. K. Bonasso and M. Moskowitz, Analysis of mammographic microcalcifications using gray-level image structure features, IEEE Transactions on Medical Imaging 15(3) (1996), 246-259.